IIETA International Information and Engineering Technology Association
Advancing the World of Information and Engineering

Journal Européen des Systèmes Automatisés
Vol. 57, No. 5, October, 2024, pp. 1359-1367
Journal homepage: http://iieta.org/journals/jesa

Energy Management Strategies of PV-Battery/Supercapacitor System for Electric Vehicles

Khaireddine Allali[1*], Abdelhak Djellad[2], Sofiane Chiheb[2], Nacer Bouderres[3], Hamza Bouzeria[1]

[1] LITE Laboratory, Department of Transport Engineering, Mentouri Brothers University Constantine 1, Constantine 25000, Algeria
[2] National Higher School of Technology and Engineering , LTSE Laboratory, Annaba 23005 Algeria
[3] LGEC Laboratory, Department of Electrical Engineering, Mentouri Brothers University Constantine 1, Constantine 25000, Algeria

Corresponding Author Email: khaireddine.allali@umc.edu.dz

https://doi.org/10.18280/jesa.570511

Received: 23 July 2024
Revised: 29 September 2024
Accepted: 10 October 2024
Available online: 28 October 2024

Keywords:
PV system, HESS, battery, supercapacitor, electric vehicle, DC-DC converter, MPPT fuzzy logic controller, EMS

ABSTRACT

The development of EVs (Electric Vehicles) as a zero-carbon alternative to fossil fuel-powered transport represents the importance of development in HESS (Hybrid Energy Storage System) and EMS (Energy Management Strategies). The present study focuses on a HESS model based on a parallel full-active configuration that integrates a (Li-ion) battery with a supercapacitor connected by two DC-DC bi-directional converters, are suitable options to power supply an electric vehicle. The EMS governing the HESS emerges as a critical element in the overall performance of EVs. The fuzzy logic control strategies have been widely used in high-level supervision and control; MPPT fuzzy logic is used for controller PV system. A complete study of the HESS; PV system, battery/supercapacitor is tested using MATLAB/Simulink. The simulation results show the performance and efficiency of the battery/supercapacitor for the EVs. Hence, the benefits of battery/supercapacitor use in a hybrid storage system are investigated and analyzed.

1. INTRODUCTION

A century later, the global automobile park has become gigantic, stabilizing in industrialized countries but exploding in emerging countries (China, India, etc.) This very significant growth in the automobile park has required governments to take action to reduce polluting emissions. At the beginning of the 1970s, the first anti-pollution standards appeared and forced car manufacturers and oil tankers to find technical solutions to reduce harmful emissions [1, 2]. Today, CO_2 emissions remain the major concern of international governments. However, this gas poses a real threat to humans and the environment. The rejection of CO_2 in the atmosphere increases each year by 2%, the road transport sector in 2020 represented 12% of the anthro pogenic greenhouse gas (GHG) emissions globally [3]. If nothing is done, we would see a doubling of these emissions by 2050. The consequences would be dramatic and irreversible for man and the environment: climate change, modifications of ecosystems, etc. [4].

Furthermore, transportation is essential to any community. Therefore, the development of a nation's social and economic systems in a balanced manner depends greatly on its transportation infrastructure. The heavy reliance of the global transportation system on fossil fuels, namely gas and oil, is one of its main issues. Transport, comprising freight and passenger travel, accounts for one-third of the total final energy consumption. This sector uses fossil fuels [5].

Hence, oil remains the most consumed primary energy in the world and the transport sector is clearly the main sector of activity for the use of petroleum products. In a context where primary energy resources are dwindling, it is essential to find ways to reduce this consumption. One of the solutions, other than using biofuels, is the introduction of photovoltaic solar energy, which allows for certain autonomy and reduces fuel consumption [1, 6]. For our country, Algeria has an excellent breeding ground, which places it in good position for the exploitation of clean and sustainable solar energy [7].

However, solar energy is a clean, limitless, free, and environmentally beneficial energy source that is also sustainable. It is therefore very crucial to use it to give energy to EVs because it is highly efficient and does not pollute the environment. The startling state of global warming forces the complete implementation of a transportation system powered by renewable energy. More application and a way to use green energy are made possible by the vehicle's utilization of solar energy. The quantity of carbon dioxide that cars produce would be drastically reduced if such a vehicle became commonplace, as would the need for oil [8, 9].

In recent years, as part of its energy transition and fight against climate change, Algeria has been moving towards electric vehicles. Solar vehicles have many advantages over conventional vehicles powered by fossil fuels. Firstly, they use a renewable and clean energy source, which is solar energy, which significantly reduces greenhouse gas emissions and helps fight climate change. In addition, solar energy is an inexhaustible resource, unlike limited fossil fuels. This means

that solar vehicles are not dependent on oil price fluctuations and can offer greater economic stability [8].

This research presents a HESS utilizing batteries and supercapacitors. The integration of supercapacitors into HESS for EVs has garnered significant interest from researchers and is viewed as a viable solution, as indicated in the literature review [10-13]. Lithium-ion batteries have been shown in a number of published studies to have a lower power density despite having a higher energy density than other rechargeable batteries [14-16]. Many approaches existing in the literature developing hybrid supply for electric vehicle using solar energy. Raut et al. [17] have studied several batteries topologies with supercapacitor using Matlab/Simulink simulation. The results have shown that the passive topology was the most suitable for the simulated system. Salama and Vokony [18] have focused on hybrid storage using a battery and superconducting coil. A fuzzy logic controller (FLC) has been implemented to manage the charging and discharging of superconducting coils and the battery with the PV system. Zhu et al. [19] have presented the power management and sizing guidelines for an EV supplied by a battery-supercapacitor (HESS). The optimization strategy for the HESS is done to reduce the battery degradation and its costs.

Since the PV system requires a reliable power storage system, and the electric vehicle requires a power supply adaptable with transients of the motor, we have simulated our electric vehicle with using Li-ion battery storage (high energy density) or with supercapacitor storage (high power density with quick response to instantaneous transients) and this to evaluate the efficiency of each system. In our paper, the simulation of electric vehicle supplied by PV panel with Hybrid Energy Storage System (HESS) composed of Li-ion battery and supercapacitor. The novelty of our paper is the energy management strategies proposed to ensure efficient function of each component (Li-ion battery and supercapacitor) which permit an optimal operating for electric vehicle, prolong its lifespan, reduce the cost of components replacement and reduce damages caused by transients. We note that the used MPPT algorithm is the fuzzy logic. The remainder of this paper is organized as follows: Section 2 provides a description of an electric vehicle system. Section 3 describes the hybrid energy storage system and their modelling. In Section 4, the flowchart of the algorithm for the system management is elaborated. The discussion of the simulation results is illustrated in Section 5. Section 6 briefs about the conclusions and future scope.

2. SYSTEM'S CONCEPTION

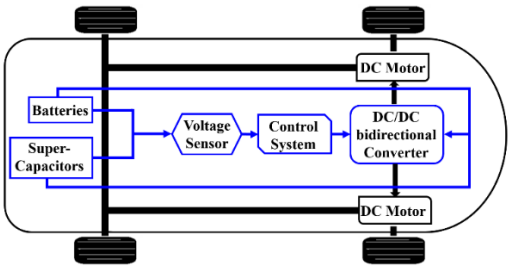

Figure 1. Hybrid EV system

Figure 1 shows the principal idea of our system; it is an electric vehicle with two-wheel drive by two direct current motors with permanent magnet, two DC motors connected with the vehicle rear wheels, batteries and supercapacitors for energy supply coupled by DC-DC bi-directional converter. Hence, the system is subjected to control system.

3. DESCRIPTION SYSTEM AND MODELLING

The hybrid energy storage system that is suggested to be used in conjunction with a photovoltaic power system to power an electric vehicle is shown in Figure 2 [20]. The HESS topologies are categorized as passive, active, or semi-active based on how storage devices are connected to the DC Bus. A passive HESS occurs when storage devices are directly linked to the DC Bus. A semi-active HESS involves one storage device connected to the DC Bus via a bi-directional DC-DC converter. An active HESS is defined by the connection of two storage devices through bi-directional DC-DC converters to the DC Bus, as discussed in the literature [21-24].

This study employs a fully active parallel topology, utilizing two bi-directional buck-boost DC-DC converters to interface the onboard energy storage units with the DC Bus.

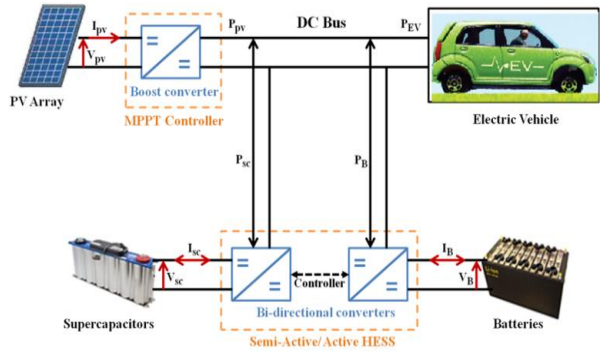

Figure 2. Schematic proposed HESS structure

The system modelling covered in this section includes the averaged state-space model of the bi-directional buck-boost DC-DC converters, the supercapacitor, the Lithium-ion battery, and the photovoltaic (PV) modules that are regulated by the fuzzy logic MPPT method.

3.1 PV panel model

The PV panels, as depicted in Figure 3, consist of several cells, each of which can be modeled as a circuit with a current source, a diode, and several resistive elements [25].

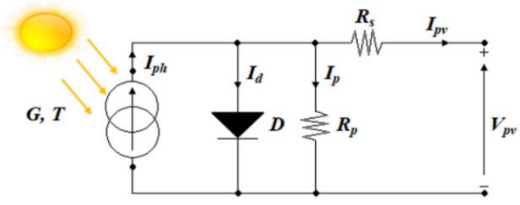

Figure 3. Equivalent circuit of PV cell [25]

The current produced by the cell is described by the following equation [26]:

$$I_{pv} = I_{ph} - I_S \times \left[exp\left(\frac{q \times (V_{pv} + R_S . I_{pv})}{A.K.Tc}\right) - 1\right] - \left(\frac{V_{pv} + R_S + I_{pv}}{R_{sh}}\right) \quad (1)$$

where, I_{pv} and V_{pv} are the cell output current and voltage; I_{ph}: The photon current; I_s: The saturation current of the diode; R_s and R_{sh} are series and parallel resistances respectively; q: The electron charge (1.6×10^{-19} C); A: The ideality factor of the P-N junction; K: Boltzmann constant ($1.380649 \times 10^{-23}\ J.K^{-1}$); T_c: Absolute cell temperature in Kelvin (K).

The photovoltaic array modeled in MATLAB/Simulink is the SPR-315E WHT-D. The different parameters of the PV module are detailed in Table 1.

Table 1. PV panel parameters

Parameter	Value
Maximum Power (P_m)	315.072 W
Voltage at MPP (V_{mp})	54.7 V
Current at MPP (I_{mp})	5.76 A
Open Circuit Voltage (V_{oc})	64.6 V
Short-Circuit Current (I_{sc})	6.28 A
Cells Number (Ns)	96

This panel, under Standard Test Conditions (STC: G=1 kW/m², T=25°C), can provide a power output Pm of 315.072 w, which corresponds to a terminal voltage Vmp of 54.7 V.

3.2 MPPT fuzzy logic control

The fuzzy logic controller is based on fuzzy strategy logic defined with sentences rather than equations. Fuzzy controller inputs are signal error (e) and error variation (Δe), so to get control (u) as controller output, the latter is considered a fuzzy linguistic variable.The operating principle of the fuzzy logic control is schematized in Figure 4 [27].

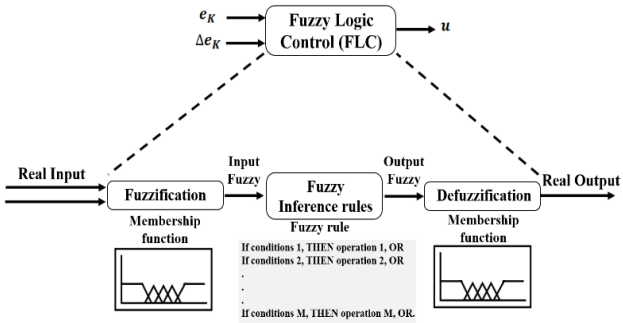

Figure 4. Fuzzy logic controller structure [27]

The fuzzy logic controller consists of three parts: fuzzification, the inference rules and defuzzification.

3.2.1 Fuzzification

The process involves transforming the physical input variables into fuzzy sets and splitting the error (e) and variation of the error (Δe) at the sampled time instances (k) into two inputs, which are specified as follows [27]:

$$e(k) = \frac{P(k) - P(k-1)}{V(k) - V(k-1)}\ with: P(k) = P(k) \cdot i(k) \quad (2)$$

$$\Delta e(k) = e(k) - e(k-1) \quad (3)$$

where, $P(k)$ and $V(k)$ are respectively the instantaneous power and voltage delivered by the PV module.

3.2.2 Inference or rules base

In this step, we try to find the relationship between input and output variables (expressed as linguistic variables). The number of these variables is determined according to the designer's choice, then a table is drawn up to define the basic operating rules of our algorithm. The sequence of our algorithm is made according to a mechanism defined on the basis rules mentioned in Table 2 and the decision is made according to these rules [27].

Table 2. Fuzzy logic basis rules

	NB	MN	NS	ZE	PS	MP	PB
NB	NB	NB	NB	NB	MN	NS	ZE
MN	NB	NB	NB	MN	NS	ZE	PS
NS	NB	NB	MN	NS	ZE	PS	MP
ZE	NB	MN	NS	ZE	PS	MP	PB
PS	MN	NS	ZE	PS	MP	PB	PB
MP	NS	ZE	PB	MP	PB	PB	PB
PB	ZE	PS	MP	PB	PB	PB	PB

where, NB: Negative Big, MN: Medium Negative, NS: Negative Small, ZE: Zero, PS: Positive Small, MP: Medium Positive, PB: Positive Big.

3.2.3 Defuzzification

After interference, fuzzy magnitudes are obtained, which need to be transformed into physical magnitudes, so a resulting membership function is defined for the output variable to perform this task. It should be noted that there are several defuzzification methods, referred to the study [27]: maxima, average of maxima and center of gravity. We should note that the latter offers the best results.

Figure 5 and Figure 6 illustrate the simulation results of MPPT using fuzzy logic for both constant and variable irradiance conditions.

The fuzzy logic control offers the ability to handle variations in inputs (Irradiance) and outputs (EV power), it can be used for solar systems of different sizes and configurations. The main thing is to establish behavioral rules in order to converge towards the optimal point of operation quickly than other algorithms.

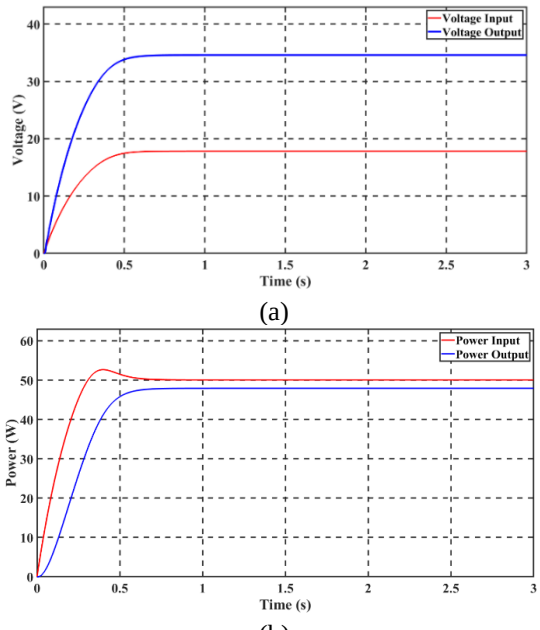

Figure 5. MPPT fuzzy logic with contant irradiance: (a) Voltage, (b) Power

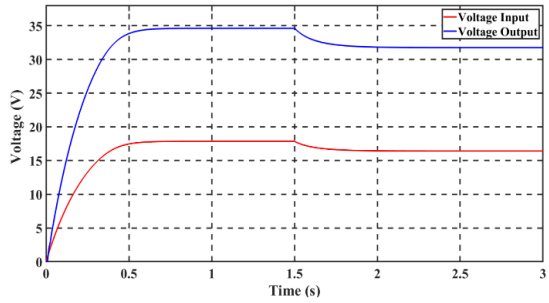

(a)

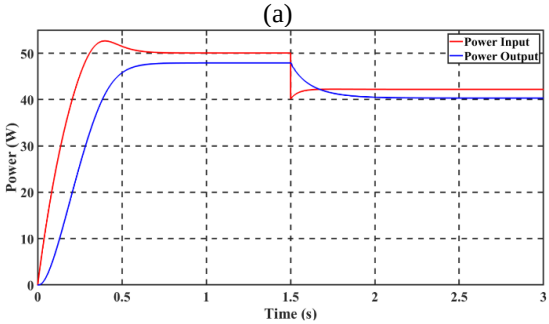

(b)

Figure 6. MPPT fuzzy logic with variable irradiance: (a) Voltage, (b) Power

3.3 Lithium-ion battery modelling

This study utilizes a general lithium-ion battery model, chosen for its simplicity and widespread availability in MATLAB/Simulink. The charge, discharge cycles and the state of charge (SOC) are modelled as follows [12]:

Charge mode (i* < 0):

$$V_{B\_ch} = E_0 - K.\frac{Q}{0.1\cdot Q+it}\cdot i^* - K\cdot\frac{Q}{Q-it}\cdot it + Ae^{-B\cdot it} \quad (4)$$

Discharge mode (i*>0):

$$V_{B\_disch} = E_0 - K.\frac{Q}{Q+it}\cdot i^* - K\cdot\frac{Q}{Q-it}\cdot it + Ae^{-B\cdot it} \quad (5)$$

$$SOC(\%) = 100\cdot\left(1 - \int\frac{i(t)dt}{Q}\right) \quad (6)$$

where, V_B is the battery voltage (V), E_o is the battery constant voltage (V), K is the polarization constant (V/Ah), Q is the maximum battery capacity (Ah), i is the battery current (A), A is the exponential voltage (V), B is the exponential capacity (Ah^{-1}), and i^* is the filtered current representing the low frequency dynamics (A).

The battery block that is being used comes from MATLAB/Simulink. It's a generic dynamic model that has been parameterized to reflect the most often used rechargeable battery types. The equivalent circuit is depicted in Figure 7 [12, 28].

The battery simulated is of lithium nickel manganese cobalt oxide (NMC) type. The parameters values of the model can be obtained from the discharge characteristic depicted in Figure 8. Therefore, the parameters values implemented in the simulation of the Li-ion battery model are as follows: E_0=216.8718 V, R=0.14388 Ω, K=0.1078 V/Ah, A=16.7952 V, B=4.3929 Ah^{-1} [12].

Figure 8 demonstrates that a discharge curve is generally segmented into three distinct sections. The initial section shows an exponential decline in voltage as the battery discharges. This area is variable in width, contingent upon the battery type. The second section denotes the charge that can be extracted from the battery until the voltage falls below the battery's nominal voltage. Lastly, the third section denotes the battery's complete discharge, which occurs when the voltage swiftly decreases.

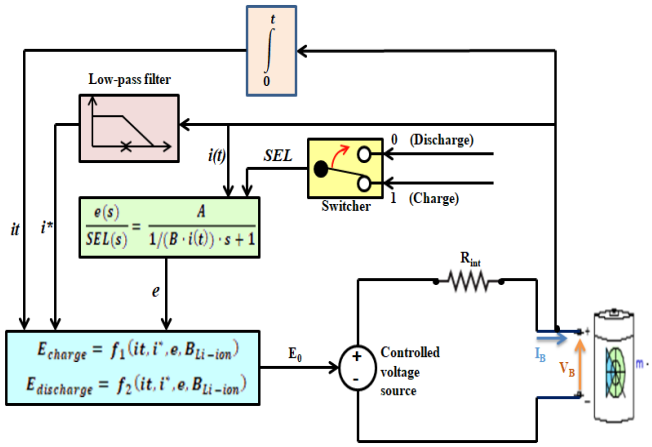

Figure 7. Dynamic battery model [12, 28]

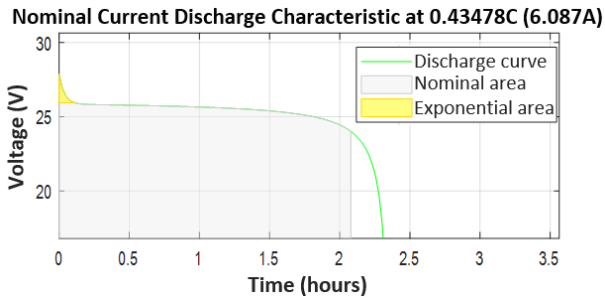

Figure 8. Battery discharge characteristic [12]

Using the accumulator data listed in Table 3, the simulations aim to charge and then discharge the battery at a constant current [20].

Table 3. Li-ion battery parameters

Parameter	Value
Nominal voltage	24 V
Cut-off voltage	18 V
Fully charged voltage	**27.9357 V**
Rated capacity	14 Ah
Maximum capacity	14 Ah
Nominal discharge current	6.087 A
Internal resistance	0.017143 Ω
Initial state-of-charge	50 %
Battery response time	0.1 s

3.4 Supercapacitor modelling

An RC equivalent circuit is used to represent the supercapacitor. It comprises a capacitance C, an equivalent parallel resistance R_{sh} that denotes self-discharging losses, and an equivalent series resistance R_s that denotes charging and discharging resistance. It is crucial to acknowledge that self-discharging losses are disregarded. The MATLAB/Simulink library contains the model illustrated in Figure 9. The supercapacitor output voltage Vsc and SOC equations are as follows [12, 29]:

$$V_{sc} = R_s \cdot i + \left[U_{C0} - \int_0^t \frac{i}{C} \cdot e^{t/(R_{sh} \cdot C)} dt\right] \cdot e^{t/(R_{sh} \cdot C)} \quad (7)$$

$$SOC(\%) = 100 \cdot \left(1 - \int \frac{i(t)dt}{C}\right) \quad (8)$$

where, U_{C0} is the initial voltage of the ideal capacitor (C).

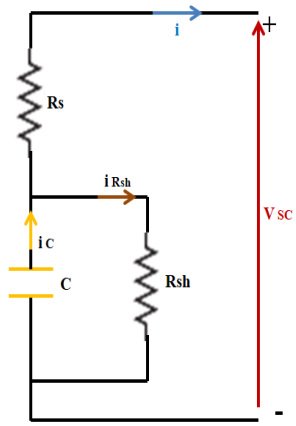

Figure 9. Supercapacitor model [12]

The parameters of supercapacitor are illustrated in Table 4 [20].

Table 4. Supercapacitor parameters

Parameter	Value
Rated voltage	32 V
Initial voltage	32 V
Equivalent series resistance	0.003 Ω
Shunt resistance	0.025 Ω
Rated capacitance	29 F
Operating temperature	25 °C

3.5 DC-DC converters modelling

As shown in Figure 2, two bi-directional buck-boost DC-DC converters connect the on-boarded sources to the DC bus. Every converter has a single source attached to it. These converters serve to control the on-board sources charging and discharging currents as well as to match the battery voltage to the DC bus. In charging mode, the bi-directional converter transfers energy from the higher voltage side (DC-bus) to the lower voltage side (ESS device) by acting as a buck converter. It performs the duties of a boost converter when discharging [30-32].

$$\text{Buck mode: } V_0 = \alpha . V_i \quad (9)$$

$$\text{Boost mode: } V_0 = V_i/(1-\alpha) \quad (10)$$

$$\text{Buck-Boost mode: } V_0 = \left(\frac{\alpha}{1-\alpha}\right) \cdot V_i \quad (11)$$

where, V_0, V_i, and α, respectively, are the output voltage, input voltage, and duty cycle of the DC-DC converter.

Figure 10 illustrates respectively the basic configuration of a DC-DC buck Figure 10 (a), DC-DC boost Figure 10 (b) and DC-DC bi-directional buck- boost converter Figure 10 (c) [24, 33, 34].

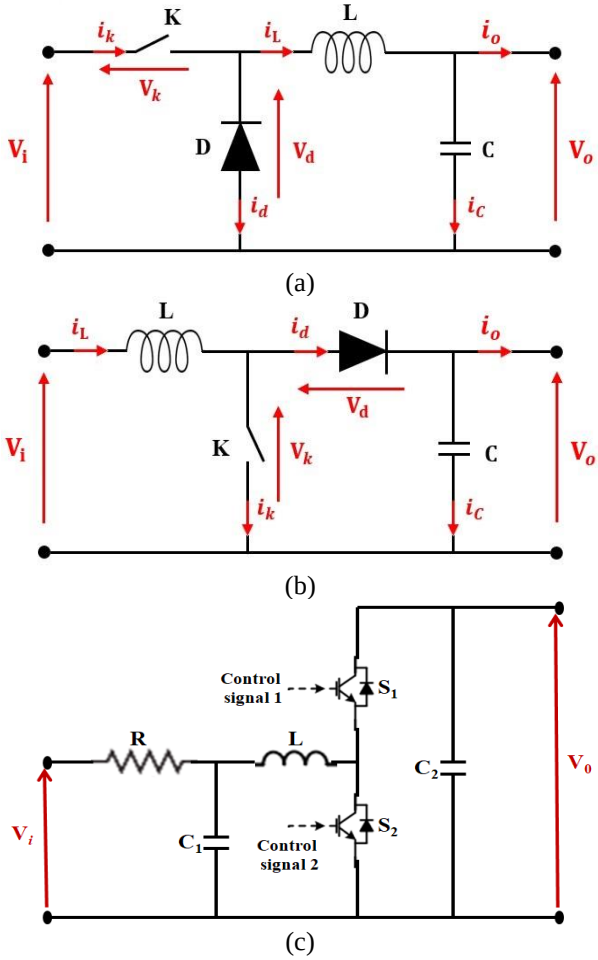

Figure 10. DC-DC converters: (a) DC-DC buck, (b) DC-DC boost, (c) DC-DC bi-directional buck- boost [33]

The parameters of the DC-DC converters are listed in Table 5.

Table 5. DC-DC converters parameters

Parameter	Boost Converter	Buck/ Boost Converter
Capacitor (mF)	100	1/1.2
Inductor (mH)	4	5
Switching frequency (kHz)	15	15

4. POWER SYSTEM MANAGEMENT

An algorithm has been developed to facilitate power management among the solar panel, batteries, and supercapacitors, taking into account environmental factors. The two modes on which the supervision algorithm is based are the Excess Power Mode (EPM), which indicates the time when the generated PV power exceeds the required EV power, and the Deficit Power Mode (DPM), which indicates the time when the generated PV power falls short of the required EV power. In this mode, there are two possible outcomes: either the EV is powered solely by the storage system in the event of insufficient solar energy, or it is powered by PV panels and storage [20, 35]. In Figure 11, the system flowchart is displayed.

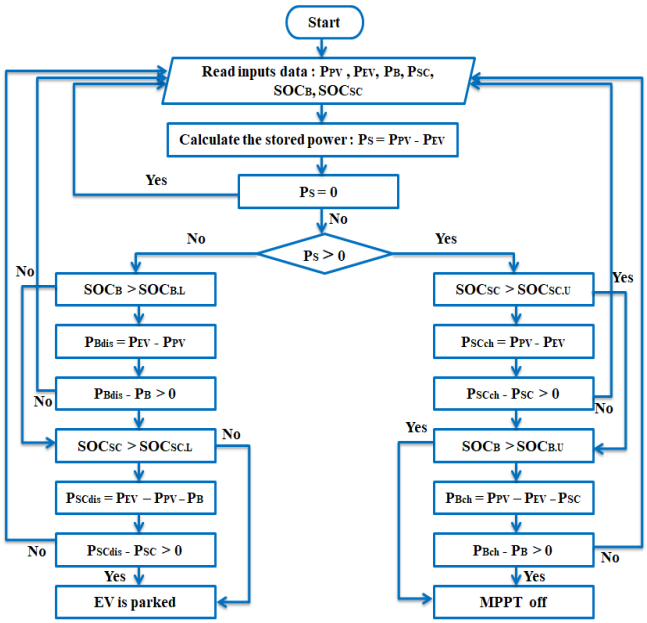

Figure 11. Flowchart of the algorithm for power system management [20]

where, P_{pv}, P_{EV}, P_S represent photovoltaique power, EV power and power stored. V_B, I_B, P_B, SOC_B represent respectively voltage, current, power and state of charge of Battery and V_{SC}, I_{SC}, P_{SC}, SOC_{SC} represent respectively voltage, current, power and state of charge of Supercapacitor.

5. RESULTS AND DISCUSSION

The simulation was conducted using MATLAB/Simulink software, based on a variable solar profile (Figure 12), a temperature of 25°C, keeping power consumption for the EV maintained constant at 500 W throughout the experiment. The characteristics of the PV panel, battery and supercapacitor used are as described above.

The results of the curves obtained for the PV panels are presented in Figure 13.

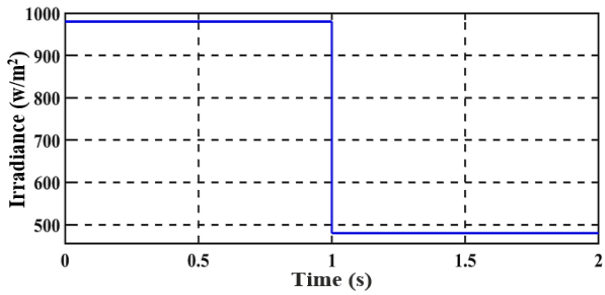

Figure 12. Solar profile

According to the curves presented in Figure 13(a), the current generated by the photovoltaic solar panel is significantly influenced by the irradiation profile used in the simulation (Figure 12). At an irradiance of 1000 W/m², the current maintains a stable value of approximately 24 A. It is important to note that this observation does not account for the initial transient phase of the simulation. When the irradiance drops to 500 W/m² at time t=1s, the current experiences a sharp decline. Subsequently, once the irradiance stabilizes at 500 W/m², the current levels off at around 13 A. Conversely, the voltage remains constant regardless of the variations in irradiance, as shown in Figure 13(b).

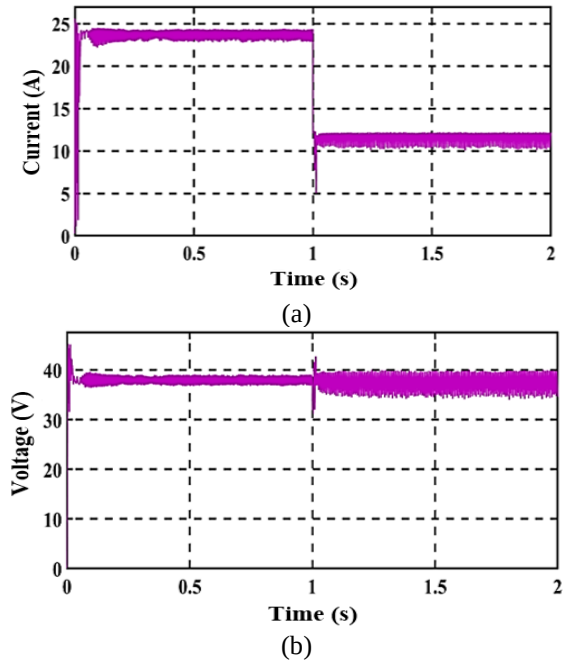

Figure 13. PV Panel output signals: (a) Current, (b) Voltage

In the present section we will study the energy management strategies in the electric vehicle. Three cases will be presented and discussed:

Cases 1: Battery storage

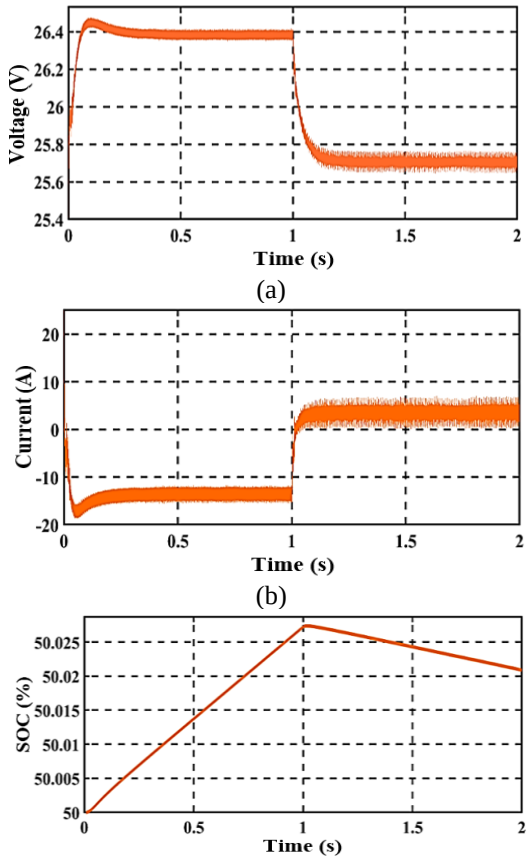

Figure 14. Battery signals: (a) Voltage, (b) Current, (c) State of Charge "SOC"

At the beginning of the simulation, the battery starts charging, increasing its state of charge from 50 % to 50.027 %. During this period, the voltage experiences fluctuations that are quickly stabilized by the regulation, ultimately reaching a value of 26.4 V. However, the current initially decreases sharply before stabilizing at approximately -13 A. Then at t = 1s, the voltage drops suddenly while the current increases due to the transition from charging to discharging. In the second phase, the battery enters discharge mode, reducing its state of charge from 50.027 % to nearly 50.020 %. During this phase, the voltage stabilizes at around 25.7 V, while the current rises and stabilizes at approximately 3 A. All of these variations are illustrated in Figure 14.

Cases 2: Supercapacitor storage

The corresponding state of charge curve indicates that the supercapacitor experienced two discharges (Figure 15): the first occurred at the beginning due to its rapid response, while the second was at time t = 1s, when both voltage (Figure 15 (a)) and current (Figure 15 (b)) reached their peak. At the end of simulation, the supercapacitor SOC is 98.92% as shown in Figure 15 (c).

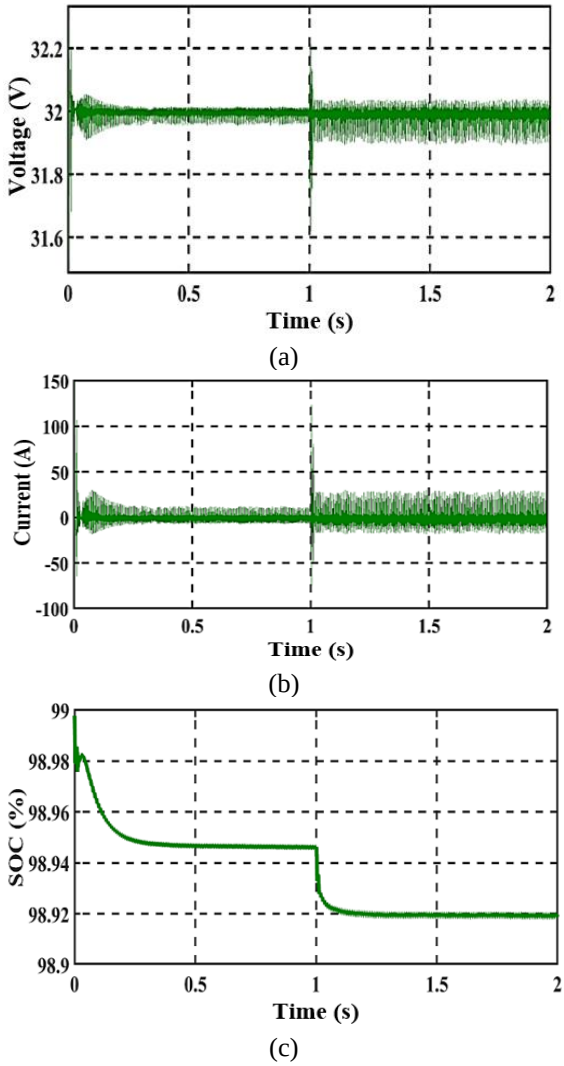

Figure 15. Supercapacitor signals: (a) Voltage, (b) Current, (c) State of Charge "SOC"

Cases 3: Battery/ Supercapacitor hybrid storage system

Figure 16 illustrates the power profiles of the PV panel; the electric vehicle and the hybrid storage system respectively.

The first curve in this figure illustrates the variation of photovoltaic power P_{pv} in accordance with the solar profile, showing a sharp decline at time t=1s, dropping from 1000 W/m^2 to 400 W/m^2. This value is below the requirement of the electric vehicle (500 W). In contrast, the EV power curve P_{EV} remains constant throughout the simulation, with only slight fluctuations as irradiance decreases, indicating the involvement of the storage system during this phase. We note that the incorporation phase of the storage system haven't evoke a significant disturbance in the EV power, where the transition have been made softly, since the energy management strategy have optimized the power injected between supercapacitor (during 0.1 s) while the battery ensuring the rest required power after that period. The power curves of the hybrid storage system support this observation, as the battery power is negative in the first phase [0; 1 s], indicating it is in charging mode. Subsequently, it shifts to discharge mode in the second phase to compensate for the long-term power deficit of P_{pv}. The supercapacitor engages first during the power peak due to its specific characteristics (high energy density and rapid response time), effectively addressing the power deficit over a short period. On the other hand, the speed of passing between supercapacitor and battery is related to the converter parameters, where the current injected by supercapacitor must do not exceed the switching element characteristics (transient current and transient voltage).

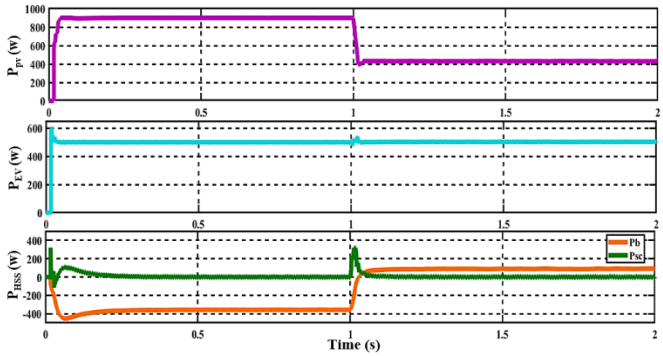

Figure 16. Power curves for a HESS

6. CONCLUSIONS

In conclusion, this paper has thoroughly examined a hybrid PV-battery/supercapacitor system supplying electric vehicle, detailing energy management strategies for a fully active configuration off grid. The PV system power has been optimized using MPPT based on fuzzy logic algorithm. The developed system was simulated using MATLAB/Simulink, allowing for an in-depth analysis. Our study case was focusing on electric car with constant power supplied by PV panel exposed to variable irradiation, and this to illustrate the participation of the battery, supercapacitor and both (battery and supercapacitor) to supply the EV during PV power interruption. The objective is highlighting characteristics of batteries and supercapacitors to propose a hybrid energy management system exploring the characteristics and improve the system lifespan. For battery case, the results have shown a slight decrease in the voltage while the current decreases sharply. When supplying the EV by supercapacitor, remarkable oscillations have appeared for current and voltage and this when a part of EV energy is supplied by the supercapacitor. Our simulation results indicate that the

battery/supercapacitor combination significantly enhances performance and efficiency for EVs with incorporating the energy management system. This HESS effectively combines the strengths of both modules, mitigating the negative impact of current fluctuations on the battery and extending its operational lifespan. Such characteristics are crucial for the effective implementation of HESS. Moreover, the HESS serves not only to protect batteries from harmful current spikes but also functions as an efficient energy storage solution for EVs. By capturing energy during braking, the HESS can notably improve the overall efficiency of electric vehicles. While the duration of action for each parameter (battery/supercapacitor) was not studied even for several PV power changes. Future work will further study the EV with variable load (taking road profile into consideration) with variable irradiance profile to ensure that the HESS is efficient to store the excess of energy and participate efficiently in each considered condition.

REFERENCES

[1] Du, Z.L., Lin, B.Q., Guan, C.X. (2019). Development path of electric vehicles in China under environmental and energy security constraints. Resources, Conservation & Recycling, 143: 17-26. https://doi.org/10.1016/j.resconrec.2018.12.007

[2] Shafiq, A., Iqbal, S., Habib, S., ur Rehman, A., ur Rehman, A., Selim, A., Ahmed, E.M., Kamel, S. (2022). Solar PV-based electric vehicle charging station for security bikes: A techno-economic and environmental analysis. Sustainability, 14(21): 13767. https://doi.org/10.3390/su142113767

[3] Statista. Global GHG emissions shares by sub sector. https://www.statista.com/statistics/1167298/share-ghg-emissions-by-sub-sector-sector-globally/.

[4] Rotondo, G., Prina, M.G., Manzolini, G., Sparber, W. (2024). Evaluating hourly charging profiles for different electric vehicles and charging strategies. Journal of Energy Storage, 95: 112388. https://doi.org/10.1016/j.est.2024.112388

[5] Chowdhury, N., Hossain, C. A., Longo, M., Yaïci, W. (2018). Optimization of solar energy system for the electric vehicle at university campus in Dhaka, Bangladesh. Energies, 11(9): 2433. https://doi.org/10.3390/en11092433

[6] Sinuraya, A., Sinaga, D.H., Simamora, Y., Wahyudi, R. (2022). Solar photovoltaic application for electric vehicle battery charging. Journal of Physics: Conference Series, 2193(1): 012075. https://doi:10.1088/1742-6596/2193/1/012075

[7] Bouraiou, A., Necaibia, A., Boutasseta, N., Mekhilef, S., Dabou, R., Ziane, A., Sahouane, N., Attoui, I., Mostefaoui, M., Touaba, O. (2020). Status of renewable energy potential and utilization in Algeria. Journal of Cleaner Production, 246: 119011. https://doi.org/10.1016/j.jclepro.2019.119011

[8] Brandon, K., Ryan, M., Aldo, G., Eric, G., Brian, S., Nnadozie, N., Michael, L., Nicolau, M. (2017). Solar powered electric vehicle. department of mechanical and civil engineering. College of Engineering and Sciences, Purdue University Northwest.

[9] Mohnish, S., Swikriti, G., Nagarjun, B.M., Harsha, R., Ramya, B.S. (2022). Design and development of solar electric vehicle with four different charging system. International Journal of Advances in Engineering and Management (IJAEM), 4(9): 1421-1427. https://doi.org/10.35629/5252-040914211427

[10] Kouchachvili, L., Yaïci, W., Entchev, E. (2018). Hybrid battery/supercapacitor energy storage system for the electric vehicles. Journal of Power Sources, 374: 237-248. https://doi.org/10.1016/j.jpowsour.2017.11.040

[11] Zhang, Q., Wang, L., Li, G., Liu, Y. (2020). A real-time energy management control strategy for battery and supercapacitor hybrid energy storage systems of pure electric vehicles. Journal of Energy Storage, 31: 101721. https://doi.org/10.1016/j.est.2020.101721

[12] Mossadak, M.A., Chebak, A., Ouahabi, N., Rabhi, A., Elmahjoub, A.A. (2024). A novel hybrid PI-backstepping cascade controller for battery-supercapacitor electric vehicles considering various driving cycles scenarios. IET Power Electronics, 2024: 1-17. https://doi.org/10.1049/pel2.12697

[13] Chen, C., Ren, G. (2024). Modeling and simulation of a battery/supercapacitor hybrid power source for electric vehicles. International Journal of Automotive and Mechanical Engineering, 21(2): 11176-11190. https://doi.org/10.15282/ijame.21.2.2024.1.0864

[14] Zubi, G., Dufo-López, R., Carvalho, M., Pasaoglu, G. (2018). The lithium-ion battery: State of the art and future perspectives. Renewable and Sustainable Energy Reviews, 89: 292-308. https://doi.org/10.1016/j.rser.2018.03.002

[15] Liang, J., Wen, L., Yu, X., Li, F., Cheng, H.M. (2018). Cathode materials: A key challenge for lithium ion batteries. Energy Storage Materials, 14: A1-A3. https://doi.org/10.1016/j.ensm.2018.07.027

[16] Eftekhari, A. (2017). Low voltage anode materials for lithium-ion batteries. Energy Storage Materials, 7: 157-180. https://doi.org/10.1016/j.ensm.2017.01.009

[17] Raut, K., Shendge, A., Chaudhari, J., Lamba, R., Alshammari, N.F. (2024). Modeling and simulation of photovoltaic powered battery-supercapacitor hybrid energy storage system for electric vehicles. Journal of Energy Storage, 82: 110324. https://doi.org/10.1016/j.est.2023.110324

[18] Salama, H.S., Vokony, I. (2020). Comparison of different electric vehicle integration approaches in presence of photovoltaic and superconducting magnetic energy storage systems. Journal of Cleaner Production, 260: 121099. https://doi.org/10.1016/j.jclepro.2020.121099

[19] Zhu, T., Lot, R., Wills, R.G., Yan, X. (2020). Sizing a battery-supercapacitor energy storage system with battery degradation consideration for high-performance electric vehicles. Energy, 208: 118336. https://doi.org/10.1016/j.energy.2020.118336

[20] Melkia, C., Ghoudelbourk, S., Soufi, Y., Maamri, M., Bayoud, M. (2022). Battery-supercapacitor hybrid energy storage systems for stand-alone photovoltaic. European Journal of Electrical Engineering/Revue Internationale de Génie Electrique, 24: 265-271. https://doi.org/10.18280/ejee.245-605

[21] Rostami, S.M.R., Al-Shibaany, Z. (2024). Intelligent energy management for full-active hybrid energy storage systems in electric vehicles using teaching-learning-based optimisation in fuzzy logic algorithms. IEEE Access, 12: 67665-67680.

https://doi.org/10.1109/ACCESS.2024.3399111
[22] Şahin, M.E., Blaabjerg, F. (2020). A hybrid PV-battery/supercapacitor system and a basic active power control proposal in MATLAB/simulink. Electronics, 9(1): 129. https://doi.org/10.3390/electronics9010129
[23] Omakor, J., Alzayed, M., Chaoui, H. (2024). Particle swarm-optimized fuzzy logic energy management of hybrid energy storage in electric vehicles. Energies, 17(9): 2163. https://doi.org/10.3390/en17092163
[24] Tang, Y., Xie, J., Shen, Y., Sun, S., Li, Y. (2024). Energy management strategy based on model predictive control-differential evolution for hybrid energy storage system in electric vehicles. IET Electrical Systems in Transportation, 2024(1): 8840942. https://doi.org/10.1049/2024/8840942
[25] Bouderres, N., Kerdoun, D., Djellad, A., Chiheb, S., Dekhane, A. (2022). Optimization of fractional order PI controller by PSO algorithm applied to a grid-connected photovoltaic system. Journal Européen des Systèmes Automatisés, 55(4): 427-438. https://doi.org/10.18280/jesa.550401
[26] Celikel, R., Yilmaz, M., Gundogdu, A. (2022). A voltage scanning-based MPPT method for PV power systems under complex partial shading conditions. Renewable Energy, 184: 361-373. https://doi.org/10.1016/j.renene.2021.11.098
[27] Sumathi, S., Kumar, L.A., Surekha, P. (2015). Solar PV and Wind Energy Conversion Systems. Switzerland: Springer. https://doi.org/10.1007/978-3-319-14941-7
[28] Ali, N.B.S., Ghoudelbourk, S., Zerzouri, N. (2022). Battery storage system design using PWM current and voltage controllers. European Journal of Electrical Engineering, 24(4): 195. https://doi.org/10.18280/ejee.240404
[29] Lozito, G.M., Intravaia, M., Corti, F., Patrizi, G., Laschi, M., Ciani, L., Vangi, D., Reatti, A. (2024). Equivalent circuit modelling of hybrid supercapacitors through experimental spectroscopic measurements. IEEE Access, (12): 78449-78462. https://doi.org/10.1109/ACCESS.2024.3408286
[30] El Fadil, H., Giri, F. (2007). Backstepping based control of PWM DC-DC boost power converters. In IEEE International Symposium on Industrial Electronics, pp. 395-400. https://doi.org/10.1109/ISIE.2007.4374630
[31] Bouziane, Y.S., Henini, N., Tlemçani, A. (2022). Energy management of a hybrid generation system based on wind turbine coupled with a battery/supercapacitor. Journal Européen des Systèmes Automatisés, 55(5): 623-631. https://doi.org/10.18280/jesa.550507
[32] Shankara, K.H., Srikantaswamy, M., Nagaraju, S. (2024). A comprehensive study on DC-DC converter for equal current sharing and voltage stability in renewable energy resources. Journal Européen des Systèmes Automatisés, 57(2): 323-334. https://doi.org/10.18280/jesa.570202
[33] Truong, H.V.A., Trinh, H.A., Do, T.C., Nguyen, M.H., Phan, V.D., Ahn, K.K. (2024). An enhanced extremum seeking-based energy management strategy with equivalent state for hybridized-electric tramway-powered by fuel cell–battery–supercapacitors. Mathematics, 12(12): 1849. https://doi.org/10.3390/math12121849
[34] Rashid, Muhammad H. (2017). Power Electronics Handbook. Butterworth-heinemann.
[35] Ghadbane, H.E., Barkat, S., Houari, A., Djerioui, A., Abdelhak, H., Mesbahi, T. (2024). A load following energy management strategy for a battery-supercapacitor hybrid power system implemented with a PIL co-simulation approach. Smart Grids and Sustainable Energy, 9(2): 32. https://doi.org/10.1007/s40866-024-00214-4

NOMENCLATURE

HESS	Hybrid Energy Storage Systems
MPPT	Maximum Power Point Tracking
EMS	Energy Management Strategie
SOC	State of Charge
EVs	Electric Vehicles
P_{pv}	Photovoltaic power (W)
P_{EV}	EV power (W)
P_B	Power of battery (W)
P_{SC}	Power of supercapacitor (W)
P_S	Power stored (W)
C	Capacitor (F)
L	Inductor (H)

Greek symbols

α	Duty cycle of the DC-DC converter